Are *n*-alkane biomarkers in loess-paleosol sequences contaminated by post-depositional organic matter? A case study from Germany using a comparative ^{14}C and OSL dating approach

Michael Zech[a,b,*,1], Sebastian Kreutzer[b,c,2], Roland Zech[d,3], Tomasz Goslar[e], Sascha Meszner[f], Cameron McIntyre[d,4], Christoph Häggi[d,5], Timothy Eglinton[d], Dominik Faust[f], Markus Fuchs[c]

a) Institute of Agronomy and Nutritional Sciences, Soil Biogeochemistry, Martin-Luther-Universität Halle-Wittenberg, Von-Seckendorff-Platz 3, 06120 Halle (Saale), Germany
b) Department of Geomorphology and Department of Soil Physics, University of Bayreuth, Universitätsstr. 30, 95440 Bayreuth, Germany
c) Department of Geography, Justus-Liebig-University Giessen, Senckenbergstr. 1, 35390 Giessen, Germany
d) Geological Institute, Biogeoscience Group, ETH Zurich, Sonneggstr. 5, 8092, Zurich, Switzerland
e) Poznan Radiocarbon Laboratory, ul. Rubiez 46, 61-612 Poznan, Poland
f) Department of Geography, Chair of Physical Geography, Dresden University of Technology, Helmholtzstr. 10, 01069 Dresden, Germany

*) corresponding author: michael_zech@gmx.de

[1] Present address: Department of Geography, Chair of Landscape- and Geoecology, Faculty of Environmental Sciences, Dresden University of Technology, Helmholtzstr. 10, 01062 Dresden, Germany.
[2] Present address: IRAMAT-CRP2A, Université Bordeaux Montaigne, Maison de l'Archéologie, Esplanade des Antilles, 33607 Pessac Cedex, France
[3] Present address: Institute of Geography and Oeschger Centre for Climate Change Research, Biogeochemistry and Paleoclimatology Group, University of Bern, Hallerstr. 12, 3012 Bern, Switzerland.
[4] Present address: Scottish Universities Environmental Research Centre (SUERC), Rankine Avenue, Scottish Enterprise Technology Park, East Kilbride, G750QF, Glasgow, United Kingdom.
[5] Present address: MARUM – Center for Marine Environmental Sciences, University of Bremen, Leobener Str., 28359 Bremen, Germany

Abstract

There is an ongoing controversial discussion whether *n*-alkane lipid biomarkers – and organic matter (OM) of loess in general – reflect a syn-sedimentary paleoenvironmental/-climate signal or whether they are significantly affected by post-depositional "contamination", for example related to root- and rhizomicrobial activity. In order to address this issue at our study site (the Middle to Late Weichselian loess-paleosol sequence Gleina in Saxony, Germany), we determined and compared radiocarbon ages of bulk *n*-alkanes and sedimentation ages, as assessed by optically stimulated luminescence (OSL) dating.

The bulk *n*-alkanes of the four dated samples yielded calibrated ^{14}C ages ranging from 24.1 to 49.7 cal. ka BP (95.4% probability ranges). While the three uppermost *n*-alkane samples are well within the range or even slightly older than the OSL-inferred sedimentation ages, the lowermost *n*-alkane sample is slightly younger than the OSL ages. There is hence no/little evidence at our study site for *n*-alkanes in loess-paleosol sequences being significantly "contaminated" by deep subsoil rooting or microbial processes. We propose a ^{14}C isotope mass balance calculation for estimating such contaminations quantitatively. Radiocarbon dating of bulk *n*-alkanes might have great potential for Quaternary research, and we encourage further comparative ^{14}C and OSL studies.

Keywords

Loess; subsoil; soil organic matter; lipid biomarkers; *n*-alkanes; roots; rhizomicrobial; luminescence dating; radiocarbon dating

Introduction

Loess-paleosol sequences (LPS) are important terrestrial archives for reconstructing Quaternary climate and landscape history (e.g., Zöller and Faust, 2009; Frechen, 2011; Marković et al., 2011; Stevens et al., 2011; Kadereit et al., 2013; Meszner et al., 2013, Antoine et al., 2013). While biomarkers have been proven for decades to be of outstanding value as molecular fossils in marine and lacustrine sediments (Eglinton and Eglinton, 2008), they have been much less investigated in LPS (for a review see e.g., Zech M. et al., 2011b). This has several reasons, amongst others, but primarily is due to the generally very low concentration of organic matter (OM) in loess.

Only during the last decade, plant leaf wax-derived lipids, particularly long-chain *n*-alkanes, have come into focus of organic geochemists using LPS as paleoenvironmental/-climate archives (Xie et al., 2002, 2003; Zhang et al., 2006; Bai et al., 2009). The popularity of *n*-alkanes as biomarkers can be attributed to the relatively easy procedure to extract and analyse them in the laboratory, as well as their recalcitrance and the good preservation in loess. This allows obtaining results even from loess samples with low organic content. Furthermore, *n*-alkanes can be used to infer vegetation changes in terms of grasses (dominated by the *n*-alkane homologues nC_{31} and nC_{33}) versus deciduous trees (dominated by the *n*-alkane homologues nC_{27} and nC_{29})(Kirkels et al., 2013; Schäfer et al., 2016b) It may be noteworthy that soil microbial degradation can affect *n*-alkane patterns and may need to be considered in certain cases (Zech M. et al., 2009; Buggle et al., 2010; Nguyen Tu et al., 2011; Zech M. et al., 2013a; Schäfer et al., 2016a). Last but not least, the compound-specific hydrogen isotope (δ^2H) signature of *n*-alkanes and its coupling with the compound-specific oxygen isotope ($\delta^{18}O$) signature of hemicellulose-derived sugar biomarkers are emerging as highly innovative paleoclimate tools in loess research (Liu and Huang, 2005; Zech R. et al., 2013; Zech M. et al., 2013c).

A major and crucial assumption of all paleo-reconstructions based on *n*-alkanes, as well as on any other biomarker in loess, is that the *n*-alkanes are deposited syn-sedimentarily and are not "contaminated" significantly by post-depositional processes. This issue, however, has been highly disputed for several years (Wiesenberg, 2012 versus Zech M. et al., 2012a; Wiesenberg and Gocke, 2013 versus Zech M. et al. 2012b; Gocke and Wiesenberg, 2013 versus Häggi et al., 2014). Gocke et al. (2010; 2013a; 2013b) claimed that a significant overprinting of loess OM, including *n*-alkanes, occurred during the Holocene and still occurs in modern times by deep subsoil rooting and rhizomicrobial deposition even in loess distant to former roots. Given

79 that the interpretation of *n*-alkane biomarker patterns alone is not straightforward for
80 reconciling this controversy, comparative ^{14}C and optically luminescence dating (OSL) can
81 serve as elegant alternative approach. Post-depositional root/rhizomicrobial contamination
82 would result in a rejuvenation of the syn-sedimentary leaf wax-derived *n*-alkanes in loess. OSL,
83 by comparison, yields (syn-sedimentary) sedimentation ages. While ^{14}C-dating of *n*-alkanes has
84 already been proven to be a powerful tool in soil science and marine sediments (Lichtfouse and
85 Eglinton, 1995; Huang et al., 1999; Kusch et al., 2010), this method is up to now rarely applied
86 in loess research. Only recently, Häggi et al. (2014) performed compound-specific ^{14}C-dating
87 of individual *n*-alkane homologues after gas chromatography (GC) separation on a preparative
88 GC. They found the *n*-alkanes to yield ^{14}C ages that agree well with the luminescence ages for
89 the investigated LPS Crvenka in Serbia. However, those results are still awaiting verification
90 from other sites and compound-specific ^{14}C-dating is very laborious. This latter disadvantage
91 maybe overcome by ^{14}C-dating of purified bulk *n*-alkane fractions (Haas et al., 2016).
92 The aim of this study was therefore to evaluate the potential of bulk, rather than compound-
93 specific, *n*-alkane ^{14}C-dating for answering the question whether *n*-alkane biomarkers in loess
94 are primarily syn-sedimentary or whether they are significantly contaminated by
95 root/rhizomicrobial organic matter. Bulk *n*-alkanes were extracted, purified and dated for the
96 Middle to Late Weichselian LPS Gleina in Saxony, Germany. The sedimentation ages were
97 assessed by OSL dating, while the methodological limits of this approach need to be kept in
98 mind, i.e. possible age under- or overestimation due to post-depositional sediment mixing or
99 insufficient bleaching. We propose a ^{14}C isotope mass balance calculation to estimate the
100 potential post-depositional root-/rhizomicrobial contamination quantitatively.
101
102 **Material and Methods**
103
104 *The loess-paleosol sequence Gleina*
105
106 Loess and paleosol samples were collected from the LPS Gleina (51° 13’50’’ N, 13° 14’ 33’’
107 E), which is located in the Saxon Loess Region, Eastern Germany (Lieberoth, 1963; Haase et
108 al., 1970; Meszner et al., 2011). A detailed description of the stratigraphy was provided by
109 Meszner et al. (2011). In brief, the uppermost meter is built up of decalcified material
110 representing the Holocene pedogenetic impact. Major parts of the Holocene soil (Luvisol) are
111 truncated and a plough horizon (Ap-horizon) nowadays forms the topsoil. According to the pan-
112 European loess stratigraphic model suggested by Marković et al. (2015), this unit refers to S0.

Below, down to approximately 8 m depth and referring to L1LL1 according to Marković et al. (2015), six paleosols, which can be described as fossil gelic Gleysols and fossil brown tundra Gleysols, alternate with loess layers (Fig. 1A). From approximately 8 m on, there is strong evidence for accumulation of partly reworked material. In situ pedogenesis contributed to the formation of a fossil gelic Gleysol in approximately 8.5 m depth and to the formation of the decalcified so-called "Gleina complex" (defined by Lieberoth, 1963 and Meszner et al., 2013 and referring to L1SS1 according to Marković et al., 2015) in approximately 10 m depth. The underlying so-called "Lommatzsch Soil Complex" (Lieberoth, 1963) was sampled from a nearby profile (approximately 20 m) and is separated in the sketch by an unconformity.

Modern root contamination partly occurred in the upper 4.5 m of the sequence, whereas hardly any modern roots were found in the lower part of the sequence. The risk of modern lateral root contamination was minimised by setting back the exposure wall by at least half a meter over the whole height of the exposure. Few rhizoliths, presumably documenting a Holocene root contamination, were found in the fossil gelic gleysol in 2 m depth.

n-Alkane preparation, radiocarbon dating and quantification of post-depositional n-alkane contamination by roots

For radiocarbon dating of the bulk *n*-alkanes, four samples were selected from the Gleina loess-paleosol sequence, for which *n*-alkane concentrations and patterns were already investigated and published (Zech M. et al., 2013a; cf. Fig. 1 therein). The samples were chosen according to their *n*-alkane concentrations (sum of long-chain *n*-alkanes >3 μg/g) and their stratigraphic position. While the samples 15 and 19 represent a weakly developed gleysol and a loess unit, respectively, from the upper part of the Gleina section (with no signs for re-working), the samples 21 and 23 represent a weakly and a strongly developed gleysol, respectively, from the lower reworked part of the Gleina section (Fig. 1). For comparison, two approximately 160 ka old samples from LPS Tumara, NE-Siberia (Zech M. et al., 2010) and a modern litter sample were analysed as radiocarbon dead and modern reference materials, respectively (Table 1).

The *n*-alkane preparation followed the procedure described by Häggi et al. (2014). In brief, free lipids were obtained with a Dionex ASE 200 accelerated solvent extractor using dichloromethane and methanol. *n*-Alkanes were purified and eluted over aminopropyl columns. Subsequent further purification steps involved $AgNO_3$ and zeolite (Geokleen) pipette columns (McDuffee et al., 2004) and served to obtain as clean bulk *n*-alkane fractions as possible (chromatograms are shown in Fig. 2). Radiocarbon measurements were conducted on an

accelerator mass spectrometer (MICADAS, Ionplus) system at the Laboratory for Ion Beam Physics (LIP), ETH Zurich. Radiocarbon ages were converted to calendar ages using *OxCal* 4.2 (Bronk Ramsey, 2009) and the IntCal13 calibration curve (Reimer et al., 2013). Calibrated ^{14}C ages (cal. ka BP) are provided as 95.4% probability range in Table 1 and Figure 1B. All bulk *n*-alkane radiocarbon data were corrected for a vacuum line combustion blank of 0.4 ± 0.1 µg C with a fraction of modern carbon ($F^{14}C$) of 0.7 ± 0.2 (Table 1) using an isotope mass balance according to Shah and Pearson (2007).

$$F^{14}C_{corrected} = \frac{\left(F^{14}C_{uncorrected} \times mass_{sample}(in\,\mu gC) - 0.7 \times 0.4\right)}{mass_{sample}(in\,\mu gC) - 0.4)} \qquad \text{(Eqn. 1)}$$

Optically stimulated luminescence (OSL) dating

A numerical chronostratigraphy of the section Gleina was established by OSL dating using fine grain (4–11 µm) quartz separates. Eight luminescence samples, generally from loess below or above paleosols and covering the depth from 2.9 to 10.8 m, were taken during night time and prepared in the laboratory for equivalent dose (D_e) determination using standard methods for fine grain quartz dating (e.g., Fuchs et al., 2005). The OSL measurements were carried out on Risø TL/OSL DA-15 luminescence readers using blue light stimulation (470 Δ 30 nm). Signals were detected in the UV band (340 Δ 80 nm). For D_e determination on 12 aliquots per sample a standard single aliquot regenerative (SAR) protocol according to Murray and Wintle (2000) was applied using the first 0.2 s after subtracting the background from the last 4 s of the shine-down curves. SAR protocol parameters were previously deduced from test measurements and the purity of the quartz extracts was tested by infrared light (IR) stimulation. The mean D_e and its standard error for each sample were used for age calculation. For dose rate calculation the U, Th and K concentration were measured using ICP-MS (K) and thick source alpha-counting (e.g., Zöller and Pernicka, 1989). The α-effectiveness (*a*-value) was measured for each sample following the procedure described in Mauz et al. (2006) and Lai et al. (2008) and resulted in a mean *a*-value of 0.04 with a standard deviation of 0.01 (n = 8; cf. Table S1). The cosmic dose rate was calculated according to Prescott and Hutton (1994). A water content of 20 ± 5 % was used. Further methodological details on the luminescence dating are given in the supplement.

Results and Discussion

n-Alkane patterns

The *n*-alkane chromatograms of the four ^{14}C-dated *n*-alkane samples reveal a bimodal pattern (Fig. 2). The long-chain *n*-alkanes (>nC$_{25}$) are characterised by a high odd-over-even predominance (OEP), i.e. particularly the *n*-alkanes nC$_{27}$, nC$_{29}$, nC$_{31}$ and nC$_{33}$ are by far more abundant than the *n*-alkanes nC$_{28}$, nC$_{30}$ and nC$_{32}$. Such patterns are typical for leaf wax-derived *n*-alkanes (Eglinton and Hamilton, 1967; Kolattukudy, 1976). The dominance of nC$_{31}$ indicates that grasses were the main source (Maffei, 1996; Zech M. et al., 2013a; Schäfer et al., 2016b). The compounds nC$_{18}$ and nC$_{20}$ also occur in relatively high amounts; in sample 15 additionally nC$_{21}$ and nC$_{22}$ (Fig. 2). While these *n*-alkanes typically do not or hardly occur in higher plant leaf waxes (Kuhn et al., 2010), Wiesenberg et al. (2009) showed that charring of grass biomass at 400 °C to 500 °C produces such *n*-alkane patterns. Soil microorganisms are reported to produce short- and mid-chained *n*-alkanes, too (Grimalt and Albaigés, 1987; Buggle et al., 2010; Zech M. et al., 2011a). We hence conclude that apart from plant leaf waxes, also charred biomass and soil microbial biomass likely contributed to the investigated *n*-alkane fractions with short-chained *n*-alkanes serving as respective molecular markers.

^{14}C ages of the bulk n-alkane samples

Radiocarbon dating of the bulk *n*-alkane fractions of the two approximately 160 ka old samples from the LPS Tumara (Zech M. et al., 2010) yielded very low blank-corrected F^{14}C values of 0.0072 and 0.0025 (Table 1). However, due to the error propagation after Shah and Pearson (2007) the absolute errors are relatively large (0.0145 and 0.0269, respectively, resulting in relative errors >50%). According to convention, minimum ages were therefore not calculated using the corrected F^{14}C values, but twice the absolute errors (Table 1), which yielded ^{14}C *n*-alkane minimum ages of >28.4 and >23.5 ka BP. For comparison, the modern litter sample yielded a corrected F^{14}C value of 1.0234, corresponding to a ^{14}C *n*-alkane age of -185 ± 75 a BP (Table 1). Thus, the ^{14}C *n*-alkane results of the radiocarbon dead and modern reference materials corroborate the reliability of the here performed bulk *n*-alkane ^{14}C analyses.

The bulk *n*-alkanes of the four dated loess-paleosol samples from the LPS Gleina yielded blank-corrected F^{14}C values ranging from 0.028 to 0.058. This corresponds to calibrated ^{14}C ages of 32.0 ± 4.5 cal. ka BP, 27.2 ± 3.6 cal. ka BP, 38.7 ± 11.0 cal. ka BP and 33.1 ± 7.2 cal. ka BP for the samples 15, 19, 21 and 23, respectively. While the mid values suggest the occurrence of

chronostratigraphic inconsistencies/age inversions (Fig. 1B), the large 95.4% probability ranges, which are calculated according to the error propagation of Shah and Pearson (2007) and which have to be taken into account, actually do not support this first impression.

OSL ages and establishment of a chronostratigraphy for the Gleina LPS

OSL fine grain quartz ages and their D_e values are shown in Table 3 and Fig. 1. Age results are given as mean and 2-σ standard error. All age values consistently increase with profile depth and within errors no age inversion occurred. The quartz luminescence signals were bright, fast decaying and highly reproducible for the determined preheat and dose recovery tests. For all samples no significant feldspar contamination (IRSL/OSL < 1%) was detected. Consequently, the derived D_e distributions show narrow scatters (c_v ca. 5%). The dose rate (supplementary) varies between 3.1 ± 0.2 Gy/ka (BT836) and 3.5 ± 0.2 Gy/ka (BT842) showing typical values for loess deposits from this region (e.g., Kreutzer et al., 2012).

For the uppermost part of the profile (ca. 3 m up to ca. 8 m) ages between 24.5 ± 2.7 ka (BT835) and 26.6 ± 2.9 ka (BT839) indicate rapid aeolian deposition during Marine Isotope Stage 2 (MIS2, Lisiecki and Raymo, 2005). These results are in accordance with previous findings from the Saxonian Loess Region (Meszner et al., 2011; Kreutzer et al., 2012; Meszner et al., 2013). The onset of loess sedimentation at ca. 10 m was attributed to the MIS3 (BT842: 45.6 ± 5.3 ka, BT840: 39.0 ± 4.4 ka). Below a hiatus at ca. 10.2 m the sediment was dated to the early Weichselian (72.8 ± 8.1 ka BT844, MIS5a to MIS4). This hiatus has been observed for all investigated loess profiles in the Saxonian Loess Region. In contrast to other investigated loess profiles in Saxony (Ostrau, Seilitz: Kreutzer et al., 2012; Meszner et al., 2013), where the onset of loess sedimentation has been dated to ca. 30 ka (transition MIS3 to MIS2), the Gleina loess OSL ages reveal an onset of loess deposition earlier in MIS3. These findings may indicate locally favoured loess accumulation and preservation due to its special morphographic position on the northernmost boundary of loess distribution in the Saxonian Loess Region. However, although unlikely in our case, an age overestimation due to an incomplete signal resetting during secondary translocation processes cannot be fully excluded, since it is not possible to detect any incomplete signal resetting using fine grain quartz dating. On the other hand, although greatest care was taken during sampling, an age underestimation due to post-depositional mixing by bioturbation might add some uncertainty with regard to interpreting the luminescence ages. The above processes have opposite effects and might cancel each other out,

and we consider them as being covered by the provided standard errors. Further details on the luminescence dating results are provided in the supplement.

Comparison - towards a quantification of post-depositional n-alkane contamination

The comparison of the ^{14}C bulk *n*-alkane ages with the OSL ages (Fig. 1B) shows that within errors the bulk *n*-alkanes of the three uppermost samples 15, 19 and 21 are well within the range or even slightly older than the OSL-inferred sedimentation ages for the LPS Gleina. This finding contradicts the thesis of a significant post-depositional *n*-alkane contamination by roots/rhizomicrobial organic matter in loess. Especially, for sample 15 where mid-chain length (i.e. C_{20}-C_{25}) compounds present a dominant fraction, this finding has further implications. It either may indicate that the deposited charred biomass is of syn-sedimentary age or that microbial contribution of mid-chain *n*-alkanes was also syn-sedimentary and didn't affect the radiocarbon age.

Only the lowermost *n*-alkane sample 23 is slightly younger than the OSL ages (Fig. 1B). As mentioned above, an OSL age overestimation due to solifluction, cryo- or bioturbation, and incomplete signal resetting (i.e. partial bleaching) cannot be fully excluded for these sediments. Nevertheless, assuming that all OSL ages reflect sedimentation ages it could be argued that sample 23 was contaminated post-depositional by root-/rhizomicrobial-derived *n*-alkanes and is therefore too young. In order to quantify the post-depositional contamination, we estimated for this sample the syn-sedimentary $F^{14}C$ value based on the (here interpolated) OSL age (42.3 ± 7.1 ka, Table 2) according to the equation

$$F^{14}C_{\text{syn-sedimentary}} = \left(\frac{1}{2}\right)^{\frac{t}{T_{1/2}}} \qquad \text{(Eqn. 2)},$$

where t is the estimated uncalibrated ^{14}C age (assuming that OSL age = calibrated ^{14}C age and using the intercept method and the IntCal13 calibration curve of Reimer et al. (2013) and $T_{1/2}$ is the half-life time of radiocarbon (5730 a). In the same way, we estimated $F^{14}C$ for contaminating roots (Table 2). On the one hand, we suspected a more or less modern ($F^{14}C$ value of 1.0) or last decadal *n*-alkane contamination by roots/rhizomicrobial deposition. Levin et al. (1985) observed atmospheric $F^{14}C$ values of more than 1.2 from 1962 to 1985 and up to almost 2.0 $F^{14}C$ in the year 1963 due to nuclear weapon tests in the Northern Hemisphere. A $F^{14}C$ value of 1.2 can be used to estimate contamination that occurred during the last decades. On the other hand, we suspected a Holocene root/rhizomicrobial contamination and calculated according to Equation 2 the theoretical $F^{14}C$ values for three Holocene time points (3 ka, 6 ka

and 9 ka, see Table 2). This is based on the finding of Gocke et al. (2010) and Pustovoytov and Terhorst (2004) that rhizoliths in last-glacial loess are of Holocene age.

The percentage of post-depositional *n*-alkane contamination "x" was then calculated using a ^{14}C isotope mass balance approach according to the equation

$$x\ \% = \frac{F^{14}C_{corrected} - F^{14}C_{syn-sedimentary}}{F^{14}C_{post-sedimentary} - F^{14}C_{syn-sedimentary}} \qquad \text{(Eqn. 3).}$$

Confidence intervals were calculated based on the $F^{14}C$ and OSL errors (Table 2). Accordingly, a modern and last decadal root/rhizomicrobial *n*-alkane contamination of 3% (confidence interval 1–5%) or a Holocene contamination of up to 9% (confidence interval 2–14%) cannot be fully excluded for this particular sample 23.

At this point, it should be mentioned that all radiocarbon ages are relatively close to their methodological age limit, and that the errors bars are therefore relatively large. Nevertheless, our results lend further support to suggest that long-chain *n*-alkanes are not significantly contaminated by post-depositional organic matter. This is in agreement with findings from Häggi et al. (2014) based on compound-specific ^{14}C dating of *n*-alkanes (and long-chain *n*-alkanoic acids) in the LPS Crvenka, Serbia. Haas et al. (2016) also reported good agreement of ^{14}C ages from bulk *n*-alkanes with luminescence ages for the LPS Kurtak, Central Siberia. It may thus not be necessary in all cases to do compound-specific radiocarbon dating, which is very laborious and requires specialized equipment and large amounts of samples. Dating bulk *n*-alkanes, i.e. at the compound-class level, has probably great potential for future loess-paleosol research.

Conclusions

For the investigated LPS Gleina, three out of four ^{14}C bulk *n*-alkane ages are well within the range or even slightly older than the OSL-inferred sedimentation ages. Only the fourth and lowermost sample may contain in absolute worst case scenarios up to 5% of modern/last decadal root-derived *n*-alkanes or up to 14% of Holocene root-derived *n*-alkanes based on ^{14}C isotope mass balance calculations. Our results show that (i) *n*-alkane biomarkers at our study site are not significantly contaminated by depositional organic matter, (ii) short and mid-chain *n*-alkanes have also a syn-sedimentary age, and (iii) ^{14}C dating of leaf wax-derived bulk *n*-alkanes in loess-paleosols has great potential as complementary dating-tool for Quaternary

research. More comparative bulk $^{14}C_{n\text{-alkane}}$ and OSL dating studies should be performed at other study sites, ideally also covering younger loess-paleosol deposits, i.e. not so close to the radiocarbon dating limits.

The results of our study suggest that in suitable LPS, the contamination of older deposits with younger carbon is not a significant contributor to the carbon budget of the sediments. However, such an observation should be determined empirically for each study site to exclude the possibility of post-depositional movement of young carbon into older sediments.

Acknowledgements

We are very grateful for constructive discussions and comments from B. Buggle, E. Lehndorff, J. Rethemeyer and two anonymous reviewers on an earlier version of this manuscript. Part of these comments including our replies is available in an online discussion forum at http://www.biogeosciences-discuss.net/bg-2012-310/#discussion. Furthermore, we greatly acknowledge the constructive reviews and feedback provided by T. Reimann, the Associate Editor M. Lachniet, the Senior Editor N. Lancaster and an anonymous reviewer, which helped to improve this manuscript. Prof. B. Huwe and Prof. L. Zöller generously provided laboratory facilities. We thank M. Sroka for support of the laboratory work and A. Kadereit from the Luminescence Laboratory of Heidelberg for her cooperation and making more machine time available.

This study was funded by the German Research Foundation (DFG; FA 239/13-2 and DFG; ZE 844/1-1). The work of S. Kreutzer and M. Fuchs was gratefully funded by the DFG (FU 417/7-2). M. Zech and R. Zech also gratefully acknowledge the support provided by the Alexander von Humboldt-Foundation and the Swiss National Foundation (SNF 131670 and SNF 150590), respectively.

Supplement

Supplementary material is available online

References

Antoine, P., Rousseau, D.-D., Degeai, J.-P., Moine, O., Lagroix, F., Kreutzer, S., Fuchs, M., Hatté, C., Gauthier, C., Svoboda, J., Lisa, L., 2013. High-resolution record of the environmental response to climatic variations during the last interglacial-glacial cycle in Central Europe: the loess-palaeosol sequence of Dolní Věstonice (Czech Republic). Quaternary Science Reviews 67, 17–38.

Bai, Y., Fang, X., Nie, J., Wang, Y., Wu, F., 2009. A preliminary reconstruction of the paleoecological and paleoclimatic history of the Chinese Loess Plateau from the application of biomarkers. Palaeogeography, Palaeoclimatology, Palaeoecology 271, 161-169.

Bronk Ramsey, C., 2009. Bayesian analysis of radiocarbon dates. Radiocarbon 51(1), 337-360.

Buggle, B., Wiesenberg, G., Glaser, B., 2010. Is there a possibility to correct fossil n-alkane data for postsedimentary alteration effects? Applied Geochemistry 25, 947-957.

Eglinton, G., Hamilton, R., 1967. Leaf epicuticular waxes. Science 156, 1322-1334.

Eglinton, T., Eglinton, G., 2008. Molecular proxies for paleoclimatology. Earth and Planetary Science Letters 275, 1-16.

Frechen, M., 2011. Loess in Eurasia. special issue in Quaternary International 234, 1-3.

Fuchs, M., Straub, J., Zöller, L., 2005. Residual Luminescence signals of recent river flood sediments: A Comparison between quartz and feldspar of fine- and coarse-grain sediments. Ancient TL 23, 25-30.

Gocke M., Wiesenberg, G., 2013. Interactive comment on „On the stratigraphic integrity of leaf-wax biomarkers in loess-paleosols“ by C. Häggi et al.. Biogeosciences Discussions 10, C7498-C7501.

Gocke, M., Kuzyakov, Y., Wiesenberg, G., 2010. Rhizoliths in loess – evidence for post-sedimentary incorporation of root-derived organic matter in terrestrial sediments as assessed from molecular proxies. Organic Geochemistry 41, 1198-1206.

Gocke, M., Kuzyakov, Y., Wiesenberg, G., 2013a. Differentiation of plant derived organic matter in soil, loess and rhizoliths based on *n*-alkane molecular proxies. Biogeochemistry 112, 23-40.

Gocke, M., Peth, S., Wiesenberg, G., 2013b. Lateral and depth variation of loess organic matter overprint related to rhizoliths — Revealed by lipid molecular proxies and X-ray tomography. Catena 112, 72-85.

Grimalt, J., Albaigés, J., 1987. Sources and occurrence of C_{12}-C_{22} *n*-alkane distributions with even carbon-numbered preference in sedimentary environments. Geochemica et Cosmochimica Acta 51, 1379-1384.

Haas, M., Bliedtner, M., Borodynkin, I., Salazar, G., Szidat, S., Eglinton, T., Zech, R., 2016. Radiocarbon dating of leaf waxes in the loess-paleosol sequence Kurtak, Central Siberia. Radiocarbon, accepted.

Haase, G., Lieberoth, I., Ruske, R., 1970. Sedimente und Paläoböden im Lößgebiet. In " Periglazial - Löß - Paläolithikum im Jungpleistozän der Deutschen Demokratischen Republik." (Richter, H., Haase, G., Lieberoth, I., Ruske, R. ,Eds.), pp. 99-212., VEB Hermann Haack, Gotha/Leipzig.

Häggi, C., Zech, R., McIntyre, C., Zech, M., Eglinton, T.I., 2014. On the stratigraphic integrity of leaf-wax biomarkers in loess paleosols. Biogeosciences 11, 2455-2463.

Huang, Y., Li, B., Bryant, C., Bol, R., Eglinton, G., 1999. Radiocarbon dating of aliphatic hydrocarbons: a new approach for dating passive-fraction carbon in soil horizons. Soil Science Society of America Journal 63(5), 1181-1187.

Kadereit, A., Kind, C.-J., Wagner, G. A., 2013. The chronological position of the Lohne Soil in the Nussloch loess section - re-evaluation for a European loess-marker horizon. Quaternary Science Reviews 59, 67-86.

Kirkels, F., Jansen, B., Kalbitz, K., 2013. Consistency of plant-specific n-alkane patterns in plaggen ecosystems: a review. The Holocene 23, 1355-1368.

Kolattukudy, P. E., 1976. Biochemistry of plant waxes. In "Chemistry and Biochemistry of Natural Waxes." (P. E. Kolattukudy, Ed.), pp. 290-349. Elsevier, Amsterdam.

Kreutzer, S., Fuchs, M., Meszner, S., Faust, D., 2012. OSL chronostratigraphy of a loess-palaeosol sequence in Saxony/Germany using quartz of different grain sizes. Quaternary Geochronology 10, 102-109.

Kuhn, T., Krull, E., Bowater, A., Grice, K., Gleixner, G., 2010. The occurrence of short chain *n*-alkanes with an even over odd predominance in higher plants and soils. Organic Geochemistry 41, 88-95.

Kusch, S., Rethemeyer, J., Schefuß, E., Mollenhauer, G., 2010. Controls on the age of vascular plant biomarkers in Black Sea sediments. Geochemica et Cosmochimica Acta 74, 7031-7047.

Lai, Z., Zöller, L., Fuchs, M., Brückner, H., 2008. Alpha efficiency determination for OSL of quartz extracted from Chinese loess. Radiation Measurements 43, 767-770.

Levin, I., Kromer, B., Schoch-Fischer, H., Bruns, M., Münnich, M., Berdau, D., Vogel, J. C., Münnich, K. O., 1985. 25 Years of tropospheric ^{14}C observations in Central Europe. Radiocarbon 27, 1-19.

Lichtfouse, E., Eglinton, T., 1995. ^{13}C and ^{14}C evidence of pollution of a soil by fossil fuel and reconstruction of the composition of the pollutant. Organic Geochemistry 23, 969-973.

Lieberoth, I., 1963. Lößsedimentation und Bodenbildung während des Pleistozäns in Sachsen. Geologie 12, 149-187.

Lisiecki, L. E., Raymo, M. E., 2005. A Pliocene-Pleistocene stack of 57 globally distributed benthic $\delta^{18}O$ records. Paleoceanography 20, 17 PP.

Liu, W., Huang, Y., 2005. Compound specific D/H ratios and molecular distributions of higher plant leaf waxes as novel paleoenvironmental indicators in the Chinese Loess Plateau. Organic Geochemistry 36, 851-860.

Maffei, M., 1996. Chemotaxonomic significance of leaf wax alkanes in the Gramineae. Biochemical Systematics and Ecology 24, 53-64.

Marković, S., Catto, N., Smalley, I., Zöller, L., 2011. The second Loessfest (2009). special issue in Quaternary International 240, 3.

Marković, S., et al., 2015. Danube loess stratigraphy – Towards a pan-European loess stratigraphic model. Earth Science Reviews 148, 228-258.

Mauz, B., Packman, S. C., Lang, A., 2006. The alpha effectiveness in silt-sized quartz: New data obtained by single and multiple aliquot protocols. Ancient TL 24, 47-52.

McDuffee, K., Timothy, E., Sessions, A., Sylva, S., Wagner, T., Hayes, J., 2004. Rapid analysis, of ^{13}C in plant-wax *n*-alkanes for reconstruction of terrestrial vegetation signals from aquatic sediments. Geochemistry, Geophysics, Geosystems 5, Q10004, doi:10.1029/2004GC000772.

Meszner, S., Fuchs, M., Faust, D., 2011. Loess-Palaeosol-Sequences from the loess area of Saxony (Germany). E&G – Quaternary Science Journal 60, 47-65.

Meszner, S., Kreutzer, S., Fuchs, M., Faust, D., 2013. Late Pleistocene landscape dynamics in Saxony, Germany: Paleoenvironmental reconstruction using loess-paleosol sequences. Quaternary International 296, 94-107.

Murray, A. S., Wintle, A. G., 2000. Luminescence dating of quartz using an improved single-aliquot regenerative-dose protocol. Radiation Measurements 32, 57-73.

Nguyen Tu, T., Egasse, C., Zeller, B., Bardoux, G., Biron, P., Ponge, J., David, B., Derenne, S., 2011. Early degradation of plant alkanes in soils: a litterbag experiment using 13C-labeled leaves. Soil Biology and Biochemistry 43, 2222-2228.

Prescott, J. R., Hutton, J. T., 1994. Cosmic ray contributions to dose rates for luminescence and ESR dating: Large depths and long-term time variations. Radiation Measurements 23, 497-500.

Pustovoytov, K., Terhorst, B., 2004. An isotopic study of a Late Quaternary loess-paleosol sequence in SW Germany. Revista Mexicana de Ciencias Geológicas 21.

Reimer, P.J. et al., 2013. IntCal13 and MARINE13 radiocarbon age calibration curves 0-50,000 years cal BP. Radiocarbon 55(4).

Schäfer, I., Bliedtner, M., Wolf, D., Faust, D., Zech, R., 2016. Evidence for humid conditions during the last glacial from leaf wax patterns in the loess-paleosol sequence El Paraíso, Central Spain. Quaternary International 407, 64-73.

Schäfer, I., Lanny, V., Franke, J., Eglinton, T., Zech, M., Vysloužilová, B., Zech, R., 2016. Leaf waxes in litter and topsoils along a European transect. Soil 2, 551-564.

Shah, S., Pearson, A., 2007. Ultra-microscale (5-25 μg C) analysis of individual lipids by ^{14}C AMS: assessment and correction for sample processing blanks. Radiocarbon 49, 69-82.

Stevens, T., Marković, S., Zech, M., Hambach, U., Sümegi, P., 2011. Dust deposition and climate in the Carpathian Basin over an independently dated last glacial–interglacial cycle. Quaternary Science Reviews 30 (5-6), 662-681.

Wacker, L., Christl, M., Synal, H., 2010. Bats: a new tool for AMS data reduction. Nuclear Instruments and Methods in Physics Research Section B 268, 976-979.

Wiesenberg, G., 2012. Interactive comment on "Technical Note: n-Alkane lipid biomarkers in loess: post-sedimentary of syn-sedimentary?" by M. Zech et al.. Biogeosciences Discussions 9, C3541-3545.

Wiesenberg, G., Gocke, M., 2013. Reconstruction of the late Quaternary paleoenvironments of the Nussloch loess paleosol sequence—Comment to the paper published by Zech et al., Quaternary Research 78 (2012), 226–235. Quaternary Research 79, 304-305.

Wiesenberg, G., Lehndorff, E., Schwark, L., 2009. Thermal degradation of rye and maize straw: Lipid pattern changes as a function of temperature. Organic Geochemistry 40, 167-174.

Xie, S., Chen, F., Wang, Z., Wang, H., Gu, Y., Huang, Y., 2003. Lipid distributions in loess-paleosol sequences from northwest China. Organic Geochemistry 34, 1071-1079.

Xie, S., Wang, Z., Wang, H., Chen, F., An, C., 2002. The occurrence of a grassy vegetation over the Chinese Loess Plateau since the last interglacial: the molecular fossil record. Science in China, Series D 45, 53-62.

Zech, M., Andreev, A., Zech, R., Müller, S., Hambach, U., Frechen, M., Zech, W., 2010. Quaternary vegetation changes derived from a loess-like permafrost palaeosol sequence in northeast Siberia using alkane biomarker and pollen analyses. Boreas 39, 540-550.

Zech, M., Buggle, B., Leiber, K., Markovic, S., Glaser, B., Hambach, U., Huwe, B., Stevens, T., Sümegi, P., Wiesenberg, G., Zöller, L., 2009. Reconstructing Quaternary vegetation history in the Carpathian Basin, SE Europe, using n-alkane biomarkers as molecular fossils: problems and possible solutions, potential and limitations. E&G – Quaternary Science Journal 85, 150-157.

Zech, M., Krause, T., Meszner, S., Faust, D., 2013a. Incorrect when uncorrected: Reconstructing vegetation history using *n*-alkane biomarkers in loess-paleosol sequences - A case study from the Saxonian loess region, Germany. Quaternary International 296, 108-116.

Zech, M., Kreutzer, S., Goslar, T., Meszner, S., Krause, T., Faust, D., Fuchs, M., 2012a. Technical Note: n-Alkane lipid biomarkers in loess: post-sedimentary or syn-sedimentary? Biogeosciences Discussions 9, doi:10.5194/bgd-9-9875-2012.

Zech, M., Pedentchouk, N., Buggle, B., Leiber, K., Kalbitz, K., Markovic, S., Glaser, B., 2011a. Effect of leaf litter degradation and seasonality on D/H isotope ratios of *n*-alkane biomarkers. Geochimica et Cosmochimica Acta 75, 4917-4928.

Zech, M., Rass, S., Buggle, B., Löscher, M., Zöller, L., 2012b. Reconstruction of the Late Quaternary paleoenvironments of the Nussloch loess paleosol sequence, Germany, using *n*-alkane biomarkers. Quaternary Research 78, 326-335.

Zech, M., Tuthorn, M., Detsch, F., Rozanski, K., Zech, R., Zöller, L., Zech, W., Glaser, B., 2013c. A 220 ka terrestrial $\delta^{18}O$ and deuterium excess biomarker record from an eolian permafrost paleosol sequence, NE-Siberia. Chemical Geology 360-361, 220-230.

498 Zech, M., Zech, R., Buggle, B., Zöller, L., 2011b. Novel methodological approaches in loess
499 research - interrogating biomarkers and compound-specific stable isotopes. E&G –
500 Quaternary Science Journal 60, 170-187.
501 Zech, R., Zech, M., Marković, S., Hambach, U., Huang, Y., 2013. Humid glacials, arid
502 interglacials? Critical thoughts on pedogenesis and paleoclimate based on multi-proxy
503 analyses of the loess-paleosol sequence Crvenka, Northern Serbia. Palaeogeography,
504 Palaeoclimatology, Palaeoecology 387, 165-175.
505 Zhang, Z., Zhao, M., Eglinton, G., Lu, H., Huang, C., 2006. Leaf wax lipids as
506 paleovegetational and paleoenvironmental proxies for the Chinese Loess Plateau over
507 the last 170 kyr. Quaternary Science Reviews 20, 575-594.
508 Zöller, L., Faust, D., 2009. Lower latitudes loess - Dust transport past and present. special issue
509 in Quaternary International 196, 1-160.
510 Zöller, L., Pernicka, E., 1989. A note on overcounting in alpha-counters and its elimination.
511 Ancient TL 7, 11-14.

512 **List of Tables and Figures**

513

514 Table 1: Results of radiocarbon analyses for the purified bulk *n*-alkane fractions of reference
515 materials and four investigated samples from the LPS Gleina.

516

517 Table 2: ^{14}C isotope mass balance calculation for quantifying potential post-depositional
518 contamination with root-/rhizomicrobial-derived *n*-alkanes.

519

520 Table 3: OSL quartz fine grain age estimates

521

522 Fig. 1: A) Stratigraphy of the LPS Gleina. Red numbers on the stratigraphic column and filled
523 black squares, respectively, mark the position of the OSL and *n*-alkane samples. B) Age-
524 depth profiles of calibrated ^{14}C bulk *n*-alkane ages (95.4% probability ranges) and OSL
525 ages with their 2-σ error bars.

526

527 Fig. 2: GC-FID *n*-alkane chromatograms for the four radiocarbon-dated bulk *n*-alkane samples.
528 The x-axes represent the retention time in minutes; the y-axes represent the GC-FID
529 signal intensity in picoampere. The long-chain *n*-alkanes nC_{29}, nC_{31} and nC_{33} originate
530 from plant leaf waxes; the nC_{31} dominance indicates dominant grass orgin; potential
531 sources of short- and mid-chained *n*-alkanes nC_{18}, nC_{20}, nC_{21} and nC_{22} are charred and
532 soil microbial biomass.

533

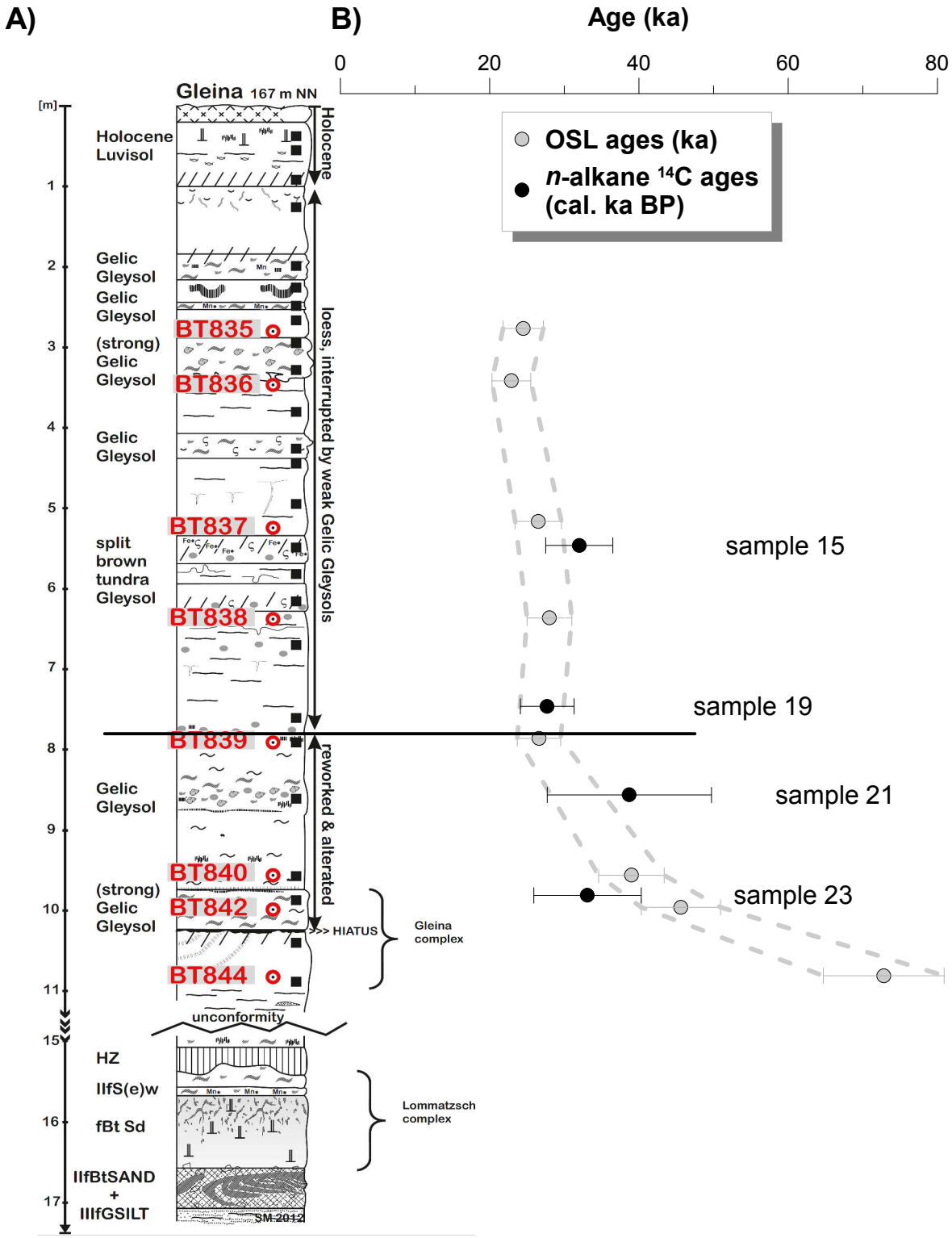
A)
B)
Age (ka)
0
20
40
60
80
Gleina 167 m NN
[m]
1
2
3
4
5
6
7
8
9
10
11
15
16
17
Holocene
Luvisol
Gelic
Gleysol
Gelic
Gleysol
(strong)
Gelic
Gleysol
Gelic
Gleysol
split
brown
tundra
Gleysol
Gelic
Gleysol
(strong)
Gelic
Gleysol
HZ
IIfS(e)w
fBt Sd
IIfBtSAND
+
IIIfGSILT
BT835
BT836
BT837
BT838
BT839
BT840
BT842
BT844
Holocene
loess, interrupted by weak Gelic Gleysols
reworked & alterated
>>> HIATUS
Gleina
complex
unconformity
Lommatzsch
complex
SM 2012
OSL ages (ka)
n-alkane 14C ages
(cal. ka BP)
sample 15
sample 19
sample 21
sample 23

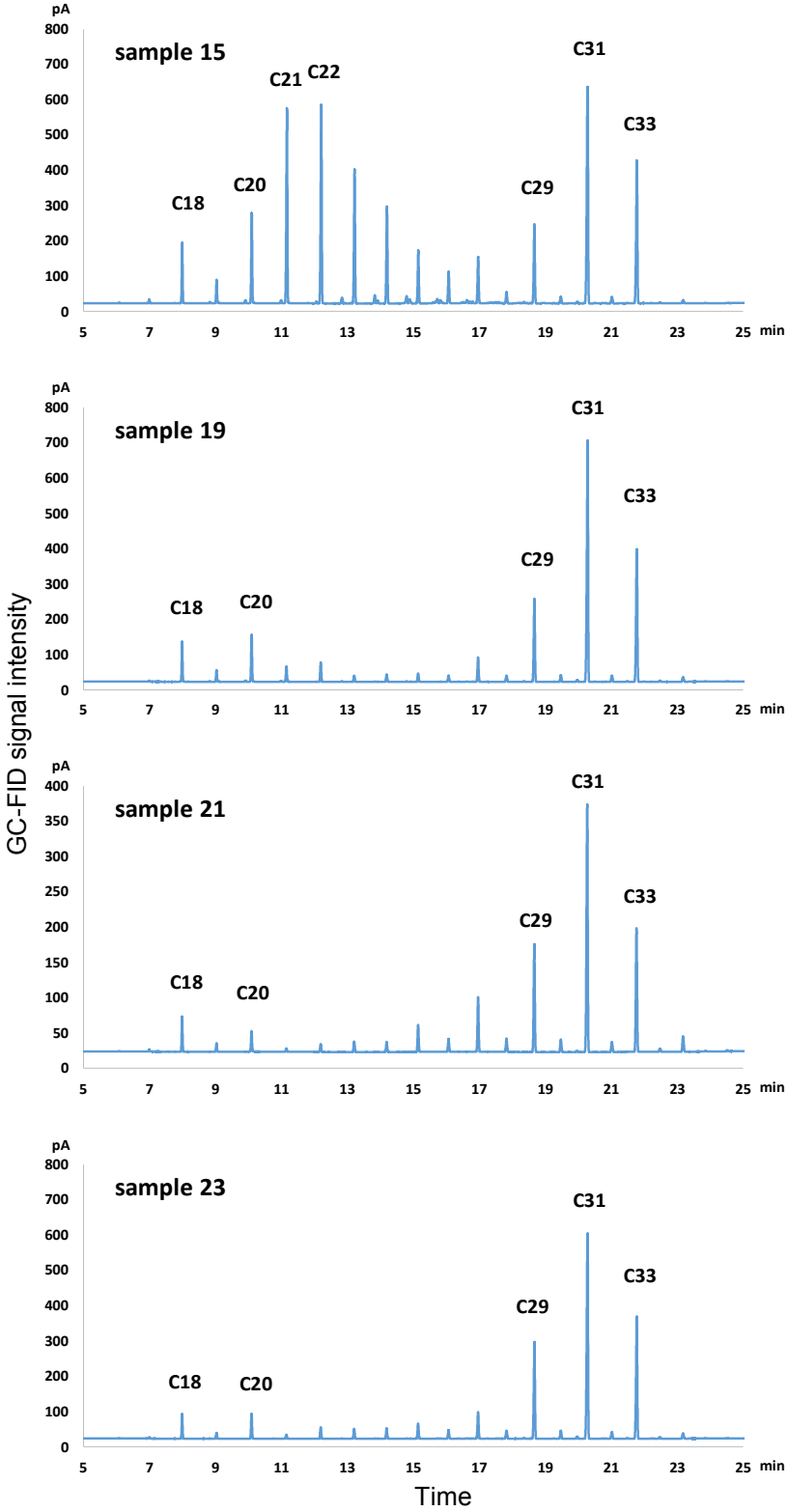
pA
sample 15
C18
C20
C21
C22
C29
C31
C33
min
sample 19
sample 21
sample 23
GC-FID signal intensity
Time

Table 1: Results of radiocarbon analyses for the purified bulk *n*-alkane fractions of reference materials and four investigated samples from the Gleina loess-paleosol sequence.

Sample name	**Lab code**	**Material:** purified bulk *n*-alkanes from	**µg C**	**$\delta^{13}C$ (‰)**	**Measured $F^{14}C$**	**Error**	**Corrected[1] $F^{14}C$**	**Error[2]**	**^{14}C Age (ka BP)**	**Error (ka)**	**Calibrated Age[3] (cal. ka BP)**
sample 12/9x	ETH 53126.1.1	~160 ka old sediments	42.9	-20.0	0.0136	0.0009	**0.0072**	0.0145[4]	>28.4	n.a.	n.a.
sample 12/9j	ETH 53127.1.1		30.3	-24.1	0.0118	0.0010	**0.0025**	0.0269[4]	>23.5	n.a.	n.a.
sample 5L	ETH 53129.1.1	modern litter	45.7	-20.8	1.0205	0.0092	**1.0234**	0.0094	-0.2	0.1	n.a.
sample 15	ETH 53125.1.1	the Gleina loess-paleosol sequence	36.4	-20.4	0.0442	0.0014	**0.0366**	0.0078	26.6	1.9	**27.5 - 36.5**
sample 19	ETH 53124.1.1		25.9	-32.0	0.0680	0.0022	**0.0581**	0.0106	22.9	1.6	**24.1 - 31.2**
sample 21	ETH 53122.1.1		26.9	-29.9	0.0387	0.0016	**0.0284**	0.0142	28.6	5.6	**27.7 - 49.7**
sample 23	ETH 53123.1.1		28.8	-27.3	0.0482	0.0017	**0.0391**	0.0105	26.0	2.5	**26.0 - 40.3**

[1] Corrected for a vacuum line combustion blank of 0.4±0.1 µg C with a $F^{14}C$ of 0.7±0.2

[2] Error propagation after Shah and Pearson (2007)

[3] Calibration done with *OxCal* 4.2 and the IntCal13 calibration curve (Bronk Ramsey, 2009; Reimer et al., 2013).

[4] Relative error >50%. Therefore, according to convention, minimum ages were not calculated using the corrected $F^{14}C$ value, but twice the absolute error.

Table 2: ^{14}C isotope mass balance calculation for quantifying potential post-depositional contamination with root-/rhizomicrobial-derived *n*-alkanes.

Sample name (depth in m)	**Corrected $F^{14}C$**	**Sedimentation OSL age (ka)**	**Estimated uncalibrated syn-sedimentary ^{14}C ages[1] (ka)**	**Syn-sedimentary $F^{14}C$[2]**	**Suspected time of contamination (ka / cal. ka BP)**	**Post-sedimentary $F^{14}C$**	**Percentage root/rhizomicrobial contamination**	**Error range based on $F^{14}C$ and OSL errors**
Sample 23 (9.8)	0.0391 ± 0.0105	42.3 ± 7.1	38.1 (31.4 - 45.9)	0.0100 (0.0039 - 0.0220)	modern	1.0000	**3%**	1 - 5%
					last decades	1.2000	**2%**	1 - 4%
					3.0 / 3.2	0.6957	**4%**	1 - 7%
					6.0 / 6.9	0.4839	**6%**	1 - 10%
					9.0 / 10.1	0.3366	**9%**	2 - 14%

[1] assuming that OSL age = calibrated ^{14}C age and using the intercept method and the IntCal13 calibration curve (Reimer et al., 2013).

[2] calculated according to equation 2.

Table 3: OSL quartz fine grain age estimates

Sample	Depth [m]	n	Fit	D_e [Gy]	Age [ka]
BT835	2.9	12/12	EXP+LIN	80.4±0.69	24.5±2.7
BT836	3.4	12/12	EXP+LIN	71.04 ±1.14	22.9±2.6
BT837	5.3	12/12	EXP+LIN	89.73±1.72	26.5±3.1
BT838	6.2	12/12	EXP+LIN	88.17±0.92	28.0±3.0
BT839	7.9	12/12	EXP+LIN	87.71±0.99	26.6±2.9
BT840	9.8	12/12	EXP+LIN	132.91±1.33	39.0±4.4
BT842	10	12/12	EXP+LIN	161.38±1.25	45.6±5.3
BT844	10.8	12/12	EXP+LIN	235.46±2.41	72.8±8.1

Note: Ages given as mean with 2-sigma uncertainty